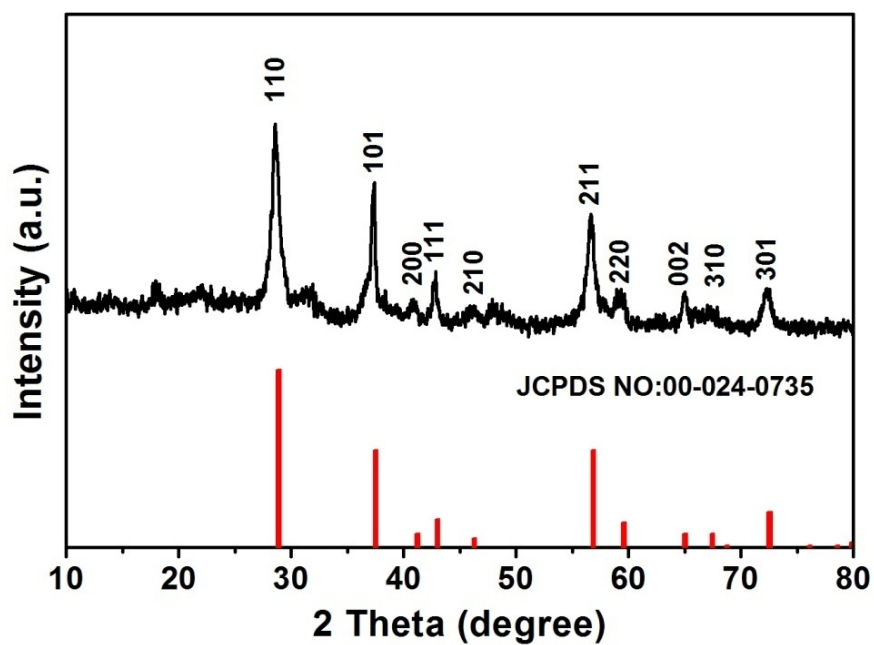


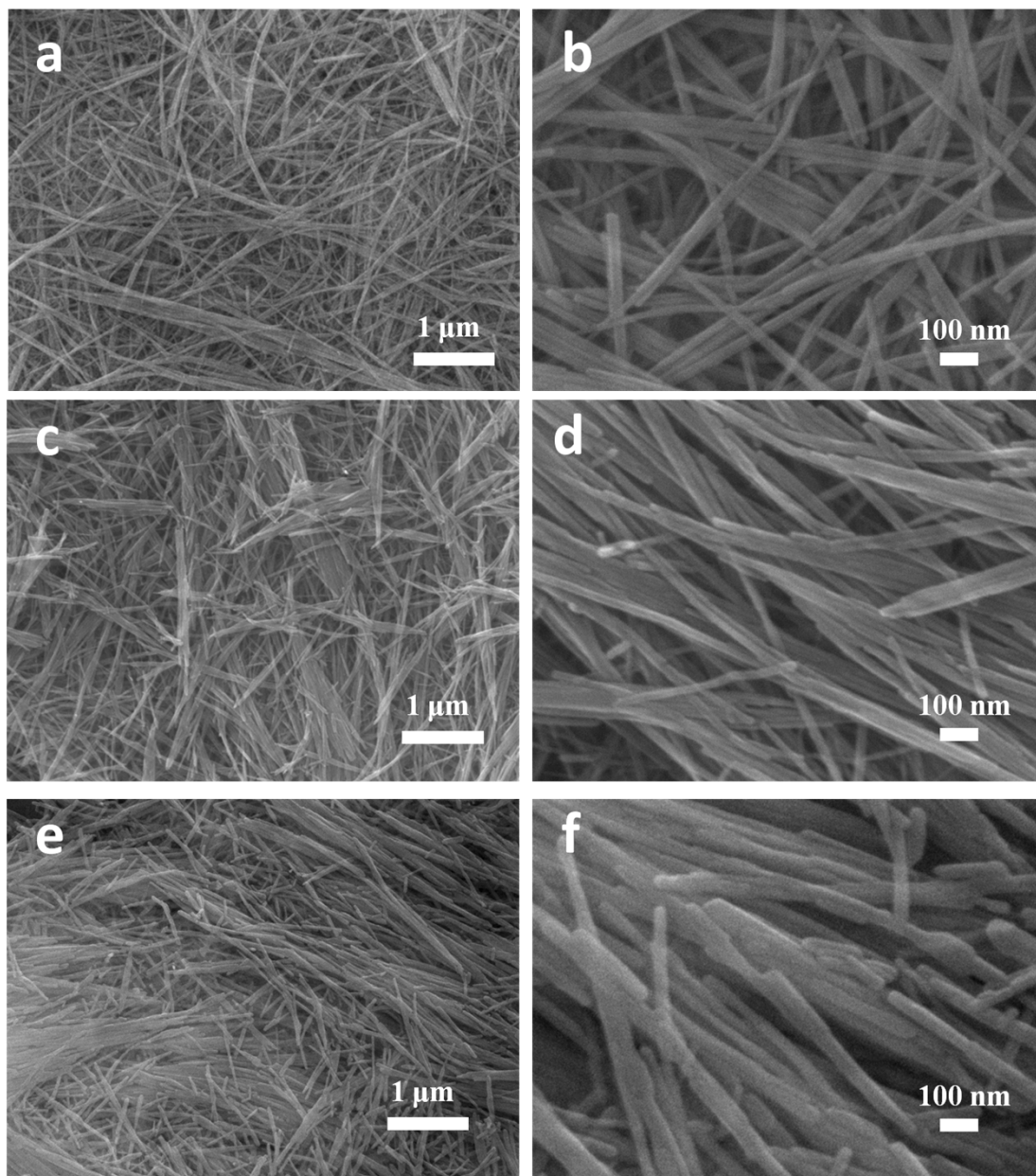
**Figure S1.** (a) XRD pattern of MnOOH nanowires. (b) SEM image of the MnOOH nanowires.

Figure S1a is the XRD pattern of MnOOH nanowires. All of the diffraction peaks can be indexed to PDF card and no other characteristic peaks from impurities are detected in the spectrum. Figure S1b shows the SEM image of the precursor MnOOH nanowires, which have diameters of 10-60 nm and smooth surfaces. SEM image shows that the morphology of the products is nanowire.



**Figure S2.** XRD pattern of MnO<sub>2</sub> nanowires.

Figure S2 is the XRD pattern of MnO<sub>2</sub> nanowires. All of the diffraction peaks can be indexed to PDF card and no other characteristic peaks from impurities are detected in the spectrum.



**Figure S3.** SEM images of (a b) MnOOH, (c d) MnO<sub>2</sub> and (e f) Li<sub>2</sub>MnO<sub>3</sub>, respectively.

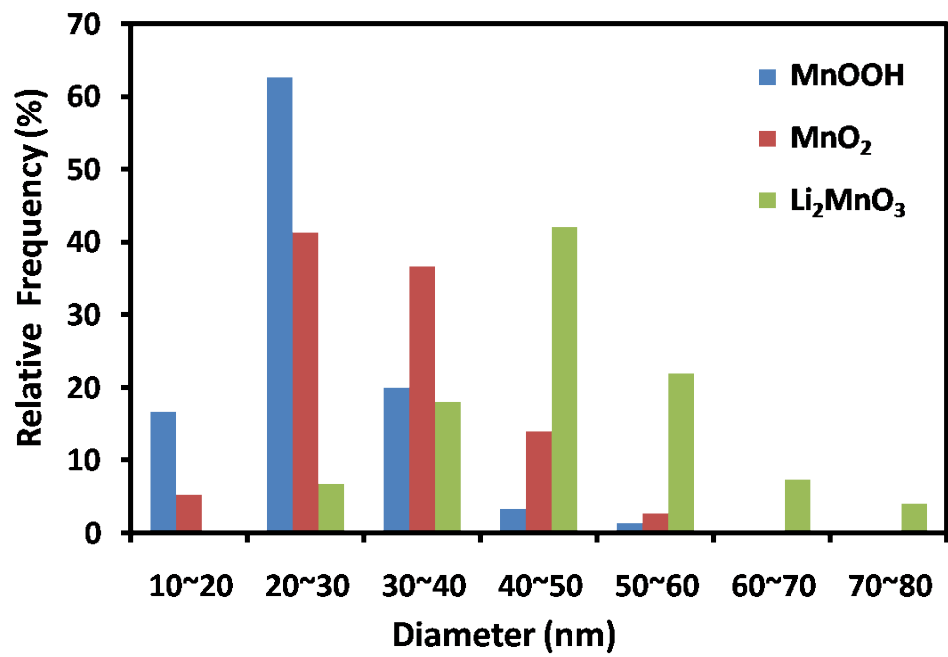


**Figure S4.** Statistical analysis of diameters of MnOOH, MnO<sub>2</sub> and Li<sub>2</sub>MnO<sub>3</sub>.



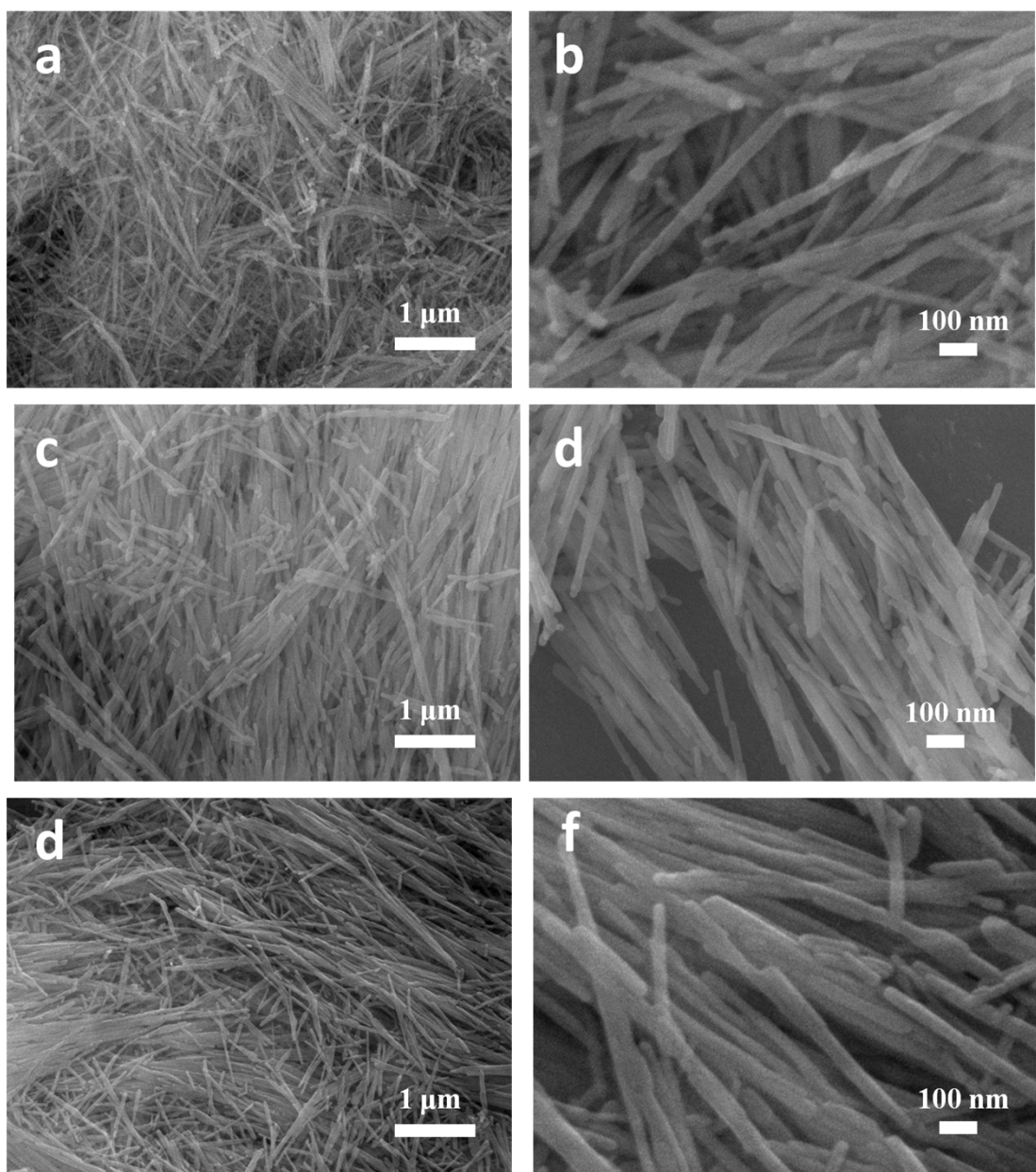


**Figure S5.** SEM images of the mixture of MnOOH precursors and LiOH annealed at 650°C for (a b) 5 h, (c d) 10 h and (e f) 15 h, respectively.

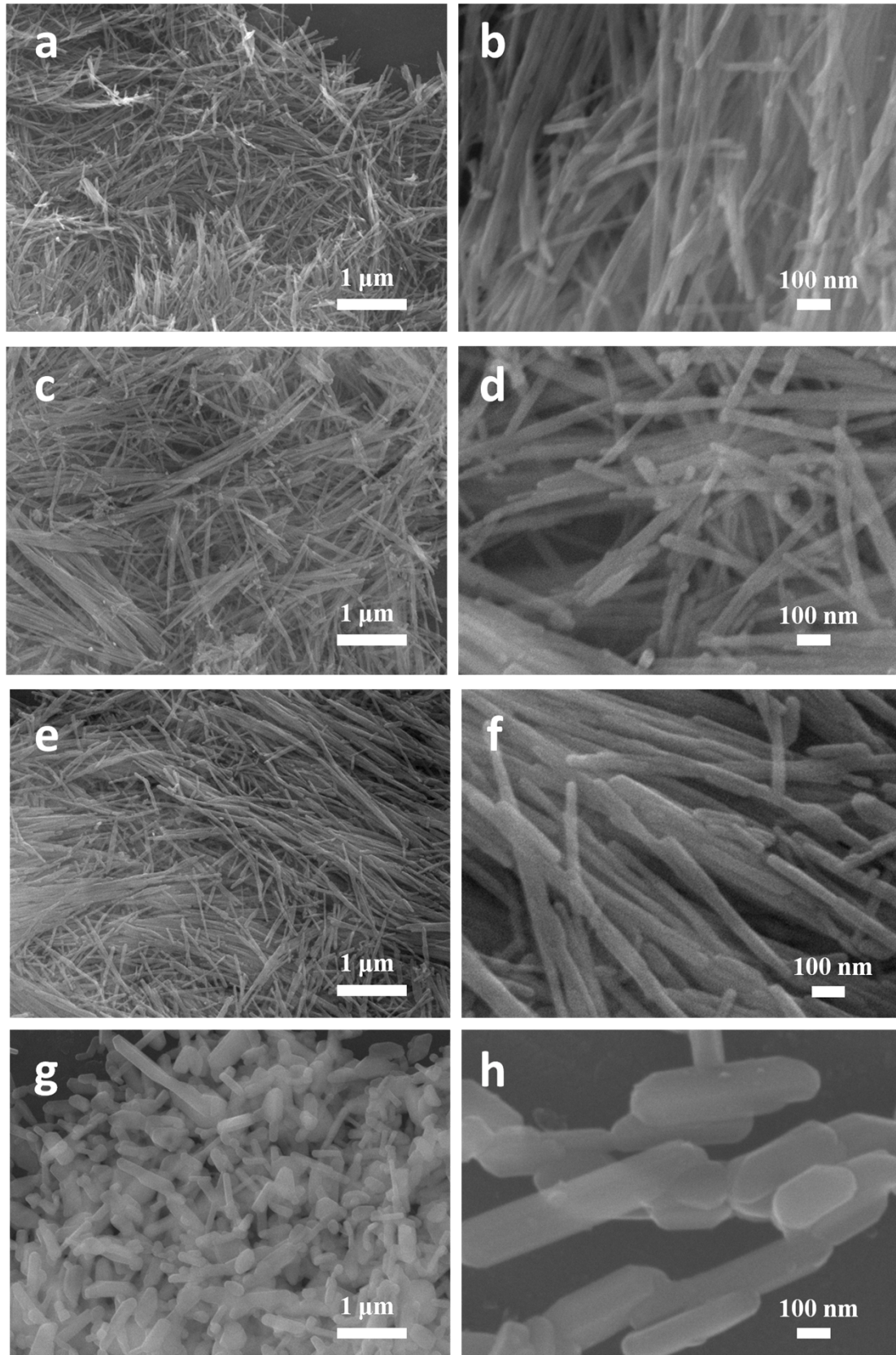


**Figure S6.** SEM images of the mixture of MnOOH precursors and LiOH annealed at (a b) 300, (c d) 500, (e f) 650 and (g h) 800°C for 15 h, respectively.

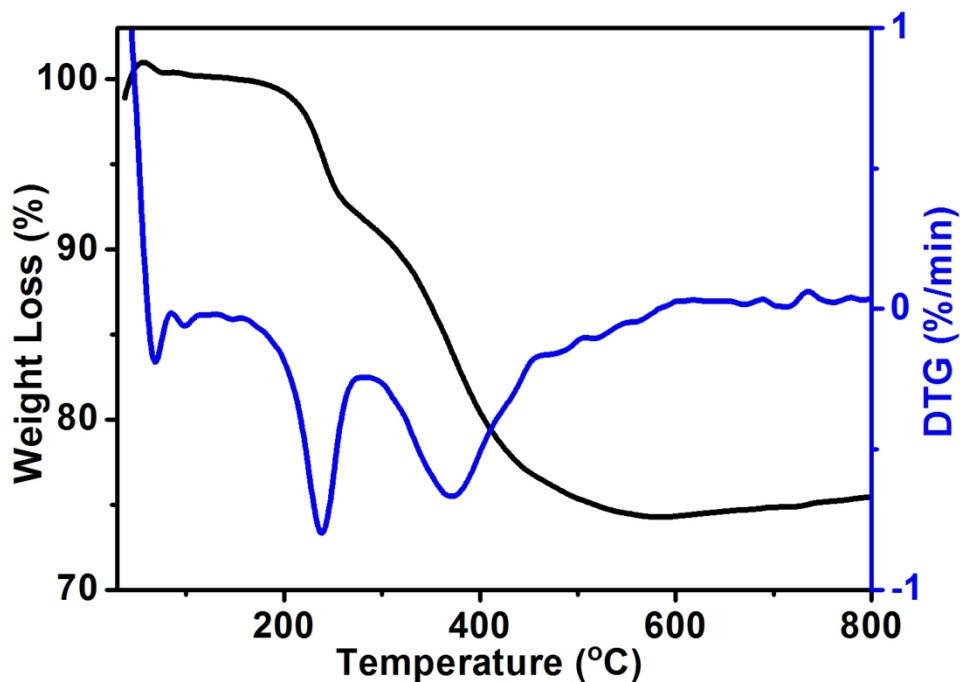


**Figure S7.** Thermogravimetric (TG) analysis of the mixture of MnOOH precursors and LiOH.

Based on the thermogravimetric (TG) analysis carried out in air by calcining the mixture of MnOOH precursors and LiOH to obtain  $\text{Li}_2\text{MnO}_3$  (Figure S7), there are three weight losses corresponding to the temperature range of  $\sim 200$  °C (I), 200-300 °C (II) and 300–600 °C (III), respectively. They are attributed to the removal of water molecules (I), the partial thermal decomposition of MnOOH to  $\text{MnO}_2$  (II) and the process from MnOOH or  $\text{MnO}_2$  to  $\text{Li}_2\text{MnO}_3$  (III), respectively. It is clear that the reaction of MnOOH to  $\text{Li}_2\text{MnO}_3$  is completed after 600 °C. Therefore, we chose the temperature of 650 °C to obtain a pure phase of  $\text{Li}_2\text{MnO}_3$ .



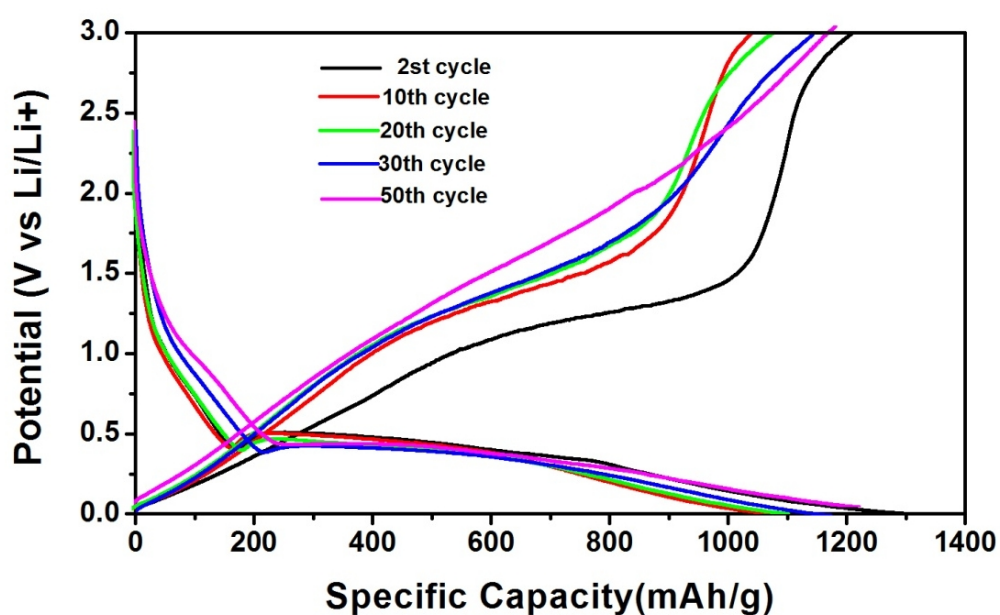


**Figure S8.** The charge–discharge curves at the current density of  $100 \text{ mA g}^{-1}$ .

Figure S8 depicts the charge/discharge potential profiles of the electrode tested at  $100 \text{ mA g}^{-1}$  at different cycles. The well-defined potential plateau is in the range of  $0.25\text{-}0.5 \text{ V}$  for lithiation and  $1.25\text{-}1.5 \text{ V}$  for delithiation. The increase in cell polarization was not observed in the case of  $\text{Li}_2\text{MnO}_3$  nanowires, not even after 50 cycles.

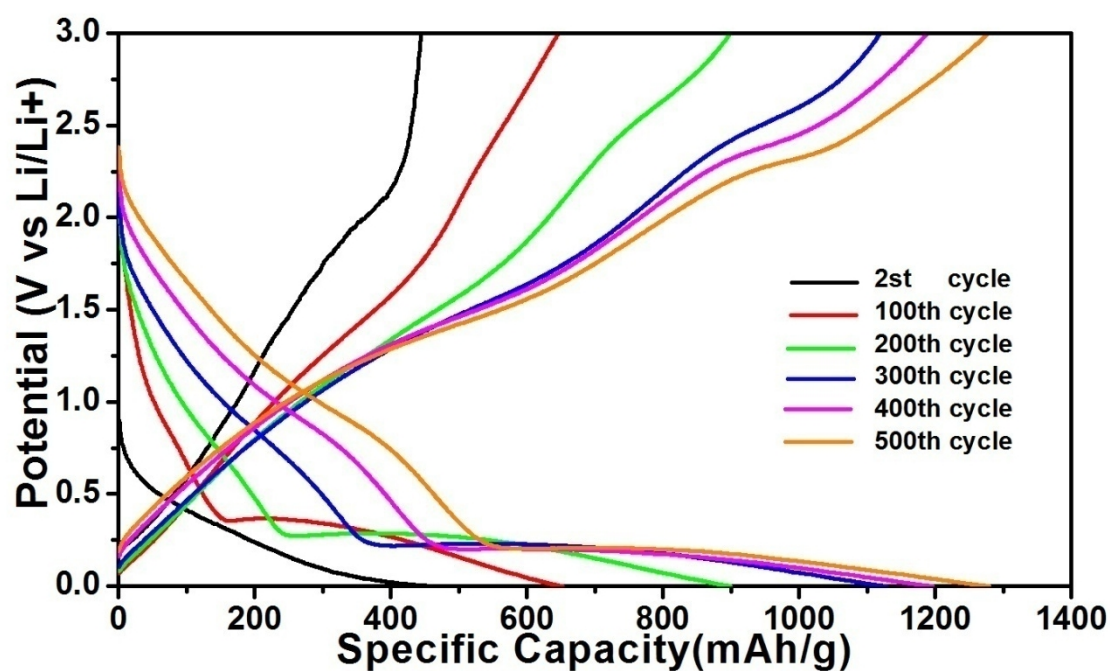


**Figure S9.** The charge–discharge curves of  $\text{Li}_2\text{MnO}_3$  nanowires at the current density of  $500 \text{ mA g}^{-1}$ .

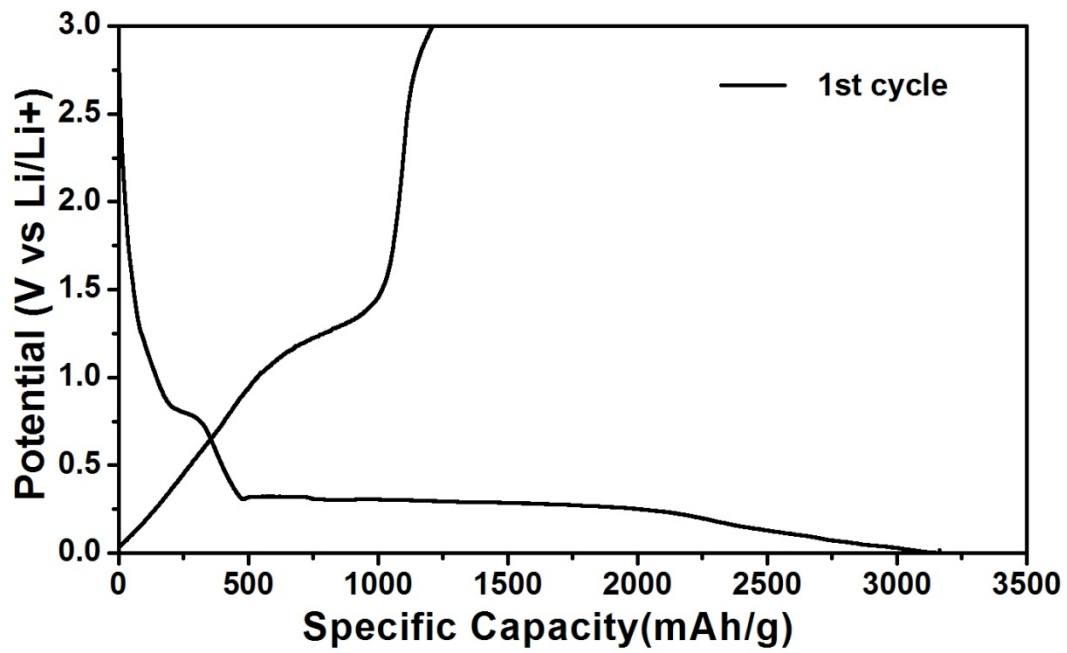


**Figure S10.** The initial charge/discharge curves of  $\text{Li}_2\text{MnO}_3$  nanowires at the current density of  $100 \text{ mA g}^{-1}$ .

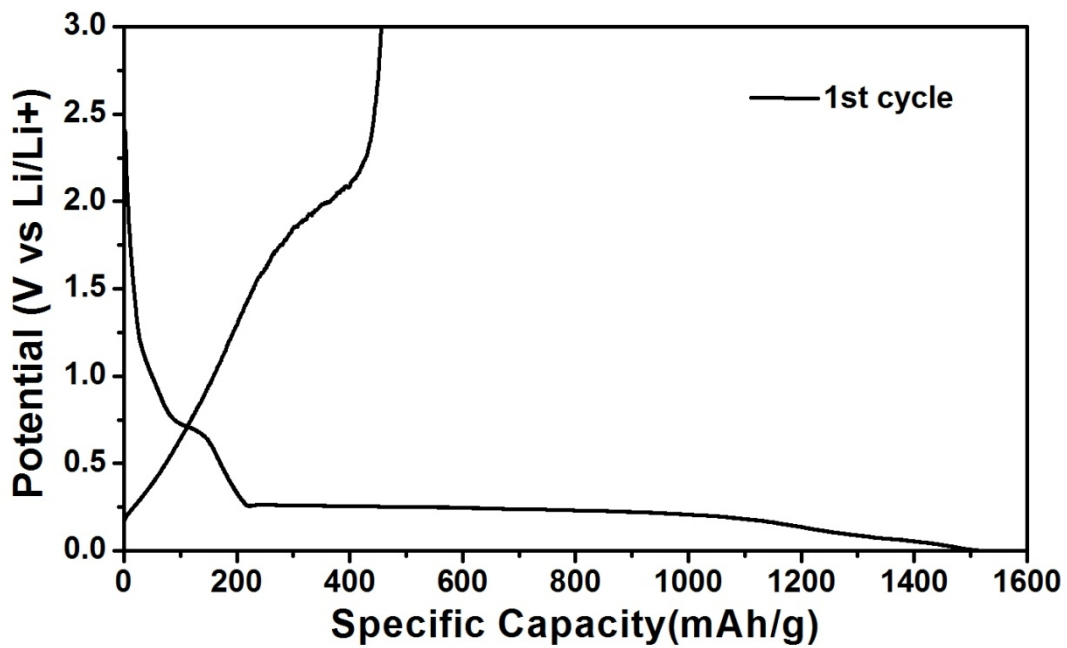


**Figure S11.** The initial charge/discharge curves of  $\text{Li}_2\text{MnO}_3$  nanowires at the current density of  $500 \text{ mA g}^{-1}$ .

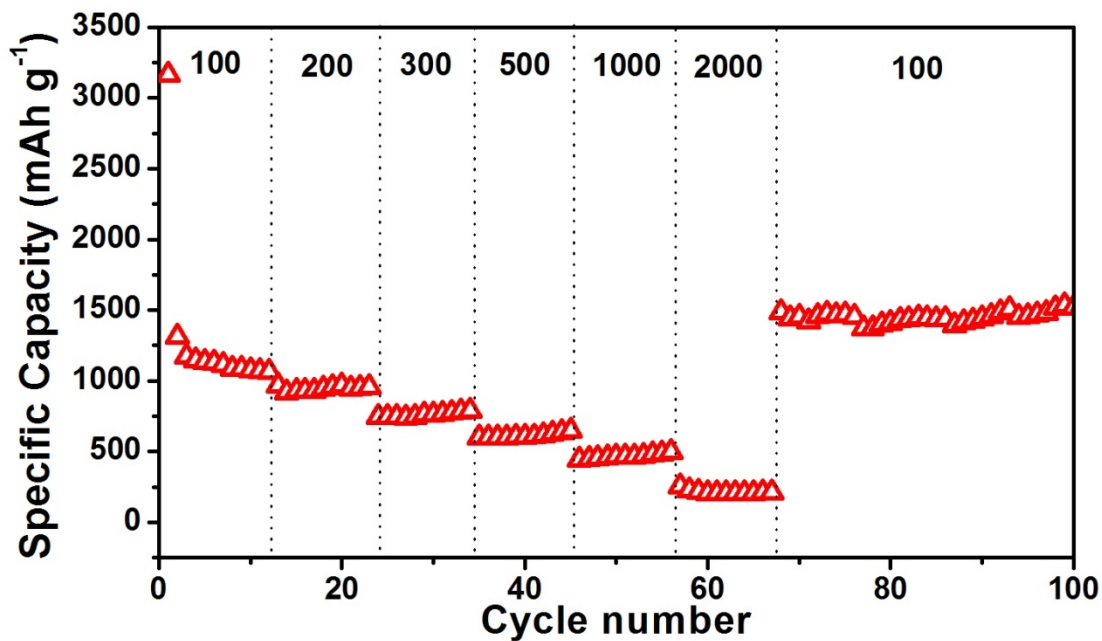


Figure S12 The rate performance of  $\text{Li}_2\text{MnO}_3$  nanowires.

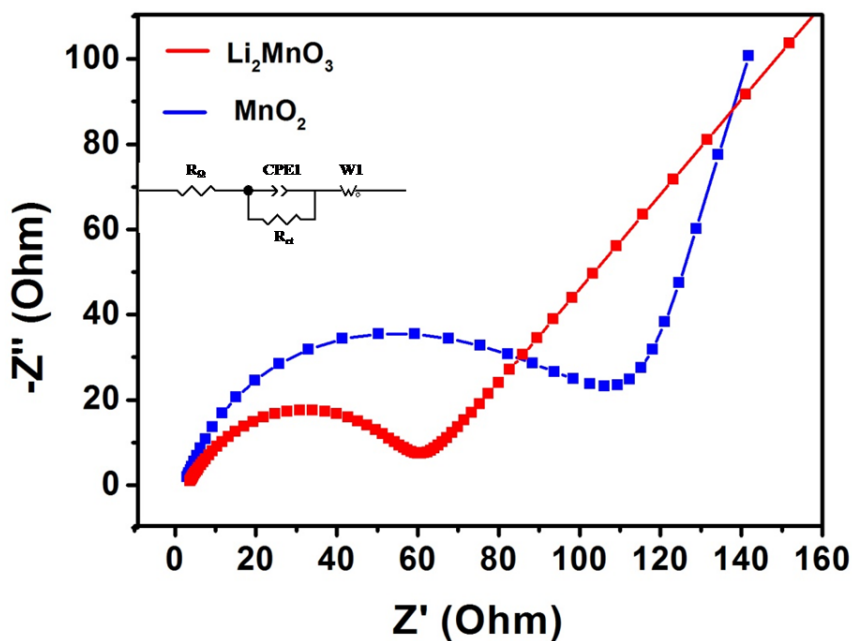
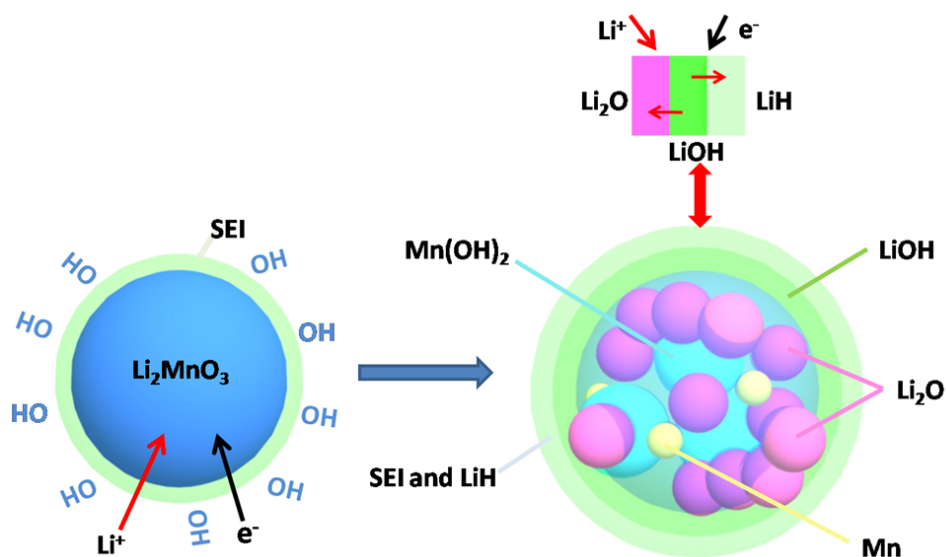


Figure S13. Nyquist plots of the AC impedance spectra for the electrodes based on the  $\text{Li}_2\text{MnO}_3$  and  $\text{MnO}_2$  nanowires.

Electrochemical impedance spectra (EIS) are measured to support the performance of the  $\text{Li}_2\text{MnO}_3$  nanowires. As shown in Figure S13, all the AC impedance spectra of the electrodes based on the  $\text{Li}_2\text{MnO}_3$  nanowires and  $\text{MnO}_2$  nanowires exhibit the typical Nyquist plots composed by a semicircle at the high-to-medium frequency region and a



slope line at the low frequency region. This semicircle is attributed to the charge transfer resistance ( $R_{ct}$ ) between the electrolyte and the electrode. The slope line might be related with the Warburg impedance ( $Z_w$ ) induced by lithium diffusion in the electrodes. The  $R_{ct}$  of  $\text{Li}_2\text{MnO}_3$  nanowires is  $52 \Omega$ , lower than the  $107 \Omega$  of  $\text{MnO}_2$  nanowires.



**Figure S14.** Summary of the reaction pathway at various states of discharge for  $\text{Li}_2\text{MnO}_3$  nanowires.

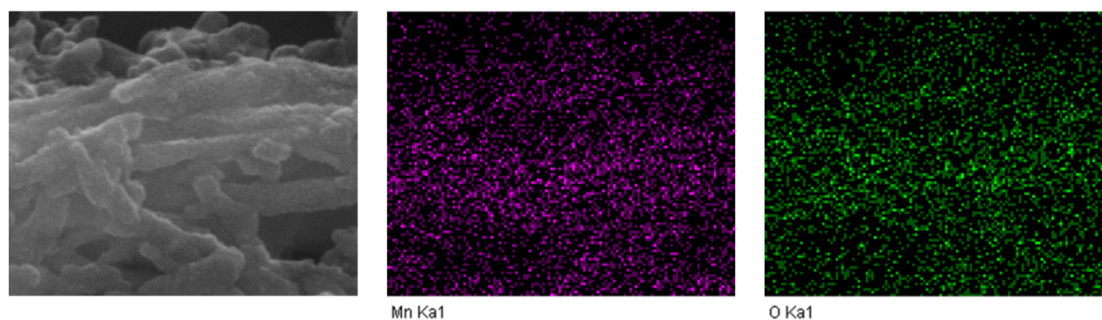


**Figure S15.** EDX elemental mappings of the cycled  $\text{Li}_2\text{MnO}_3$  nanowires.

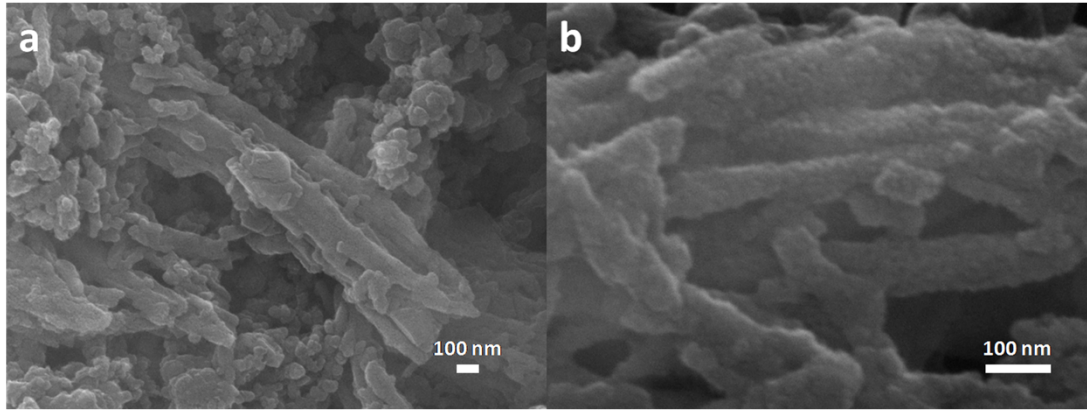


**Figure S16.** SEM images of the cycled  $\text{Li}_2\text{MnO}_3$  nanowires after 500 cycles.

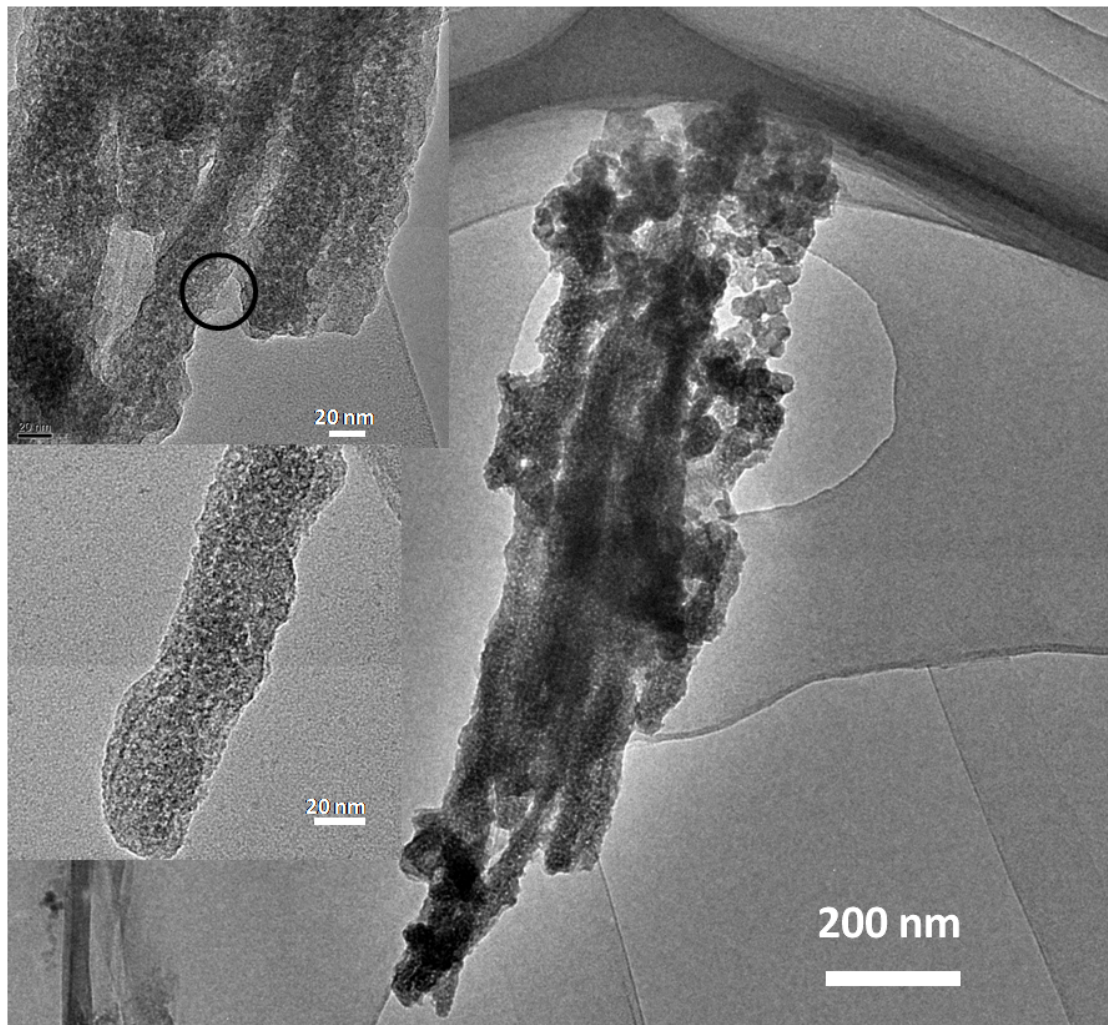


**Figure S17.** TEM images of the cycled  $\text{Li}_2\text{MnO}_3$  nanowires after 500 cycles.